SCALE AND FREQUENCY DEPENDENCE OF REFLECTION AND TRANSMISSION COEFFICIENTS

Matthias G. Imhof

Earth Resources Laboratory
Department of Earth, Atmospheric, and Planetary Sciences
Massachusetts Institute of Technology
Cambridge, MA 02139

ABSTRACT

Well-logs show that heterogeneities occur at many different spatial scales. In this paper, we want to characterize how waves are affected by these heterogeneities, and we study how reflection and transmission coefficients depend on temporal frequency and spatial scale. We use wavelet transformations to filter certain spatial scales from the velocity logs. The scale-filtered logs serve as input for a numerical layer-stack model to calculate reflection and transmission coefficients as functions of frequency and scale. We find that transmission coefficients are largely independent of frequency or scale. They depend mostly on average slowness. Contrarily, reflection coefficients are extremely sensitive to the perturbations of the slownesses, even at low frequencies.

INTRODUCTION

Seismic velocities obtained from well-logs commonly exhibit strong fluctuations over very short distances. Typically, the sampling interval is well below one meter. On the other hand, seismic properties are also estimated from surface seismic data which have a resolving power of tens of meters. Many researchers are studying how to relate the two different datasets obtained at different spatial wavelengths. We want to pose a slightly different question instead: which spatial scales of heterogeneity affect the propagation of seismic waves of a particular temporal frequency? We will answer this question by calculating reflection and transmission coefficients as functions of temporal frequency of the wave and spatial scale contents of the medium. As we will show, the results for transmission experiments differ dramatically from reflection experiments. We find that transmission is oblivious to the different spatial scales. Contrarily, reflections are extremely sensitive to change of scale content. Even perturbations at scales well below the seismic wavelength affect the resulting reflection parameters dramatically. Specifically, we will concentrate on reflection and transmission magnitudes and phases which relate to phase- and group-slownesses of the layer-stack.

METHOD

We assume that P-wave velocity $v(z)$ and density $\rho(x)$ are functions of depth, z, only. We have m layers sandwiched between regions 0 and $n = m + 1$. A schematic of the geometry and the indexing of the regions is shown in Figure 1. We assume that waves propagate acoustically along the z-direction. In each homogeneous region k, we postulate an upgoing pressure wave $A_k \exp(iq_k z)$ and a downgoing wave, $B_k \exp(-iq_k z)$ where $q_k = \omega/v_k$ is the vertical wavenumber at angular frequency ω. At each interface, e.g. between regions k and $\ell = k + 1$ located at depth d_k, we have to satisfy continuity conditions for pressure and normal displacement.

$$\begin{aligned} A_k \exp(iq_k d_k) + B_k \exp(-iq_k d_k) &= A_\ell \exp(iq_\ell d_k) + B_\ell \exp(-iq_\ell d_k) \\ A_k \frac{q_k}{\rho_k} \exp(iq_k d_k) - B_k \frac{q_k}{\rho_k} \exp(-iq_k d_k) &= A_\ell \frac{q_\ell}{\rho_\ell} \exp(iq_\ell d_k) - B_\ell \frac{q_\ell}{\rho_\ell} \exp(-iq_\ell d_k) \end{aligned} \tag{1}$$

We introduce the impedance ratio $\xi_{k\ell} = (\rho_k q_\ell)/(\rho_\ell q_k) = \xi_{\ell k}^{-1}$ to simplify the notation.

$$\begin{aligned} A_k \exp(iq_k d_k) + B_k \exp(-iq_k d_k) &= A_\ell \exp(iq_\ell d_k) + B_\ell \exp(-iq_\ell d_k) \\ A_k \exp(iq_k d_k) - B_k \exp(-iq_k d_k) &= \xi_{\ell k} \left[A_\ell \exp(iq_\ell d_k) - B_\ell \exp(-iq_\ell d_k) \right] \end{aligned} \tag{2}$$

Defining the local reflection coefficient between region k and ℓ as $R_{\ell k} = (1 - \xi_{\ell k})/(1 + \xi_{\ell k}) = -R_{k\ell}$, we can express these boundary conditions by the interaction matrix $\mathbf{V}_{\ell k}$.

$$\begin{pmatrix} A_\ell \exp(iq_\ell d_k) \\ B_\ell \exp(-iq_\ell d_k) \end{pmatrix} = \mathbf{V}_{\ell k} \cdot \begin{pmatrix} A_k \exp(iq_k d_k) \\ B_k \exp(-iq_k d_k) \end{pmatrix} \quad \mathbf{V}_{\ell k} = \frac{1}{2}(1 + \xi_{\ell k}) \begin{pmatrix} 1 & R_{\ell k} \\ R_{\ell k} & 1 \end{pmatrix} \tag{3}$$

We use the propagator matrix $\mathbf{P}_{\ell k}$ to extrapolate the pressures from interface k to interface ℓ through region ℓ.

$$\begin{pmatrix} A_\ell \exp(iq_\ell d_\ell) \\ B_\ell \exp(-iq_\ell d_\ell) \end{pmatrix} = \mathbf{P}_{\ell k} \cdot \begin{pmatrix} A_\ell \exp(iq_\ell d_k) \\ B_\ell \exp(-iq_\ell d_k) \end{pmatrix} \quad \mathbf{P}_{\ell k} = \begin{pmatrix} \exp(iq_\ell [d_\ell - d_k]) & 0 \\ 0 & \exp(-iq_\ell [d_\ell - d_k]) \end{pmatrix} \tag{4}$$

Recursively combining interactors and propagators, we relate the fields in region r to the ones in region $s > r$.

$$\begin{pmatrix} A_s \exp(iq_s d_s) \\ B_s \exp(-iq_s d_s) \end{pmatrix} = \mathbf{P}_{s(s-1)} \cdot \mathbf{V}_{s(s-1)} \cdots \mathbf{P}_{(r+1)r} \cdot \mathbf{V}_{(r+1)r} \cdot \begin{pmatrix} A_k \exp(iq_(r + 1) d_r) \\ B_k \exp(-iq_(r + 1) d_r) \end{pmatrix} \tag{5}$$

For a downward propagating wave impinging on the layer-stack, we define the total reflection coefficient $R = A_0/B_0$ and the total transmission coefficient $T = B_n/B_0$ (where $n = m + 1$) which are related by a linear system.

$$\begin{pmatrix} 0 \\ T \end{pmatrix} = \mathbf{V}_{nm} \cdot \left\{ \prod_{k=1}^{m} \mathbf{P}_{k(k-1)} \cdot \mathbf{V}_{k(k-1)} \right\} \cdot \mathbf{P}_0 \cdot \begin{pmatrix} R \\ 1 \end{pmatrix} \quad \mathbf{P}_0 = \begin{pmatrix} \exp(iq_0 d_0) & 0 \\ 0 & \exp(-iq_0 d_0) \end{pmatrix} \tag{6}$$

This system can easily be solved for R and T. Additionally, we can test the numerical accuracy through the conservation of energy: $|R|^2 + \xi_{0t}|T|^2 = 1$.

The reflection and transmission coefficients are complex valued and frequency dependent. We separate the coefficients into modulus and phase $R(\omega) = |R(\omega)| \exp\left(i\phi_p(\omega)\right)$ and $T(\omega) = |T(\omega)| \exp\left(i\psi_p(\omega)\right)$ where we use the subscript p to denote the 2π phase ambiguity. We apply a modification of Tribolet's algorithm (1977) to unwrap the true phases $\phi(\omega)$ and $\psi(\omega)$. We begin with an interval $[\omega_i, \omega_j]$ of width $2\Delta\omega = \omega_j - \omega_i$ and center-frequency $\Omega = \omega_i + \Delta\omega$. We also assume to have an estimate of the phase derivative $\phi'(\omega_i) = \partial\phi(\omega_i)/\partial\omega$ at the lower bound of the interval. We recursively bisect the interval until the extrapolated phase increases over the subinterval $\phi'(\omega_i)\Delta\omega < \pi$. The extrapolation step ensures that we will resolve the phase increase without ambiguity. However, we continue to bisect the subinterval until $|\phi_p(\omega_i) + \phi'(\omega_i)\Delta\omega - \phi_p(\Omega)| < \epsilon$ where ϵ is an arbitrary threshold. The term $\phi_p(\Omega)$ is obtained by evaluating (6) for frequency Ω. This second bisection guarantees that we do not miss a $\pm n\pi$ discontinuity ($n \in \mathbb{N}$) caused by a pol or a zero in the coefficient or a transition from one sheet in the Riemann surface to another (Poggiagliolmi *et al.*, 1982; Shatilo, 1992). We then estimate the derivative $\phi'(\omega_j)$ at the upper bound of the subinterval using $\phi_p(\omega_j)$ and $\phi_p(\Omega)$. This derivative is used to calculate the principal phases in the next interval, etc. Finally, we unwrap the phase by appropriately adding multiples of 2π until all discontinuities induced by the 2π ambiguity are removed.

We decompose the unwrapped phases further into static and dynamic components: $\phi(\omega) = \phi_0 + \omega s_p^r(\omega)$ and $\psi(\omega) = \psi_0 + \omega s_p^t(\omega)$. In addition, we calculate $s_g^r(\omega) = d\phi(\omega)/d\omega$ and $s_g^t(\omega) = d\psi(\omega)/d\omega$. Up to proportionality constants, the quantities $s_p^r(\omega)$, $s_p^t(\omega)$, $s_g^r(\omega)$, and $s_g^t(\omega)$ can be identified as frequency dependent phase- and group-slownesses of the reflected and the transmitted wavefield.

To examine the scale dependence of reflection and transmission coefficients, we scale-filter the velocity profile in the wavelet domain. We use a Haar transformation to decompose the velocity function $v(z)$ into its scale-components (Strang, 1989). In the wavelet domain, we remove certain scale components and recombine the remaining ones. The result is a new velocity function $\hat{v}(z)$ with the same average velocity but without some of the original spatial variations. Let us write $a^0 = v(z)$. We apply a highpass filter H given by $(1/2, -1/2)$ which yields the spatial high-frequency variations b^1 of a^0. The corresponding orthogonal lowpass filter L defined by $(1/2, 1/2)$ yields the remaining velocity function a^1 which is again operated on by L and H yielding a^2 and b^2, etc. The original a^0 can be reconstructed by a recursive application of the dual operator H^* and L^*.

$$a^{j+1} = La^j\,, \qquad b^{j+1} = Ha^j \tag{7a}$$

$$\tilde{a}^j = L^*\tilde{a}^{j+1} + H^*\tilde{b}^{j+1} \tag{7b}$$

Expression (7a) is one step of the decomposition into global average a^J (where $J = \log_2 m$) and the different scales b^j. Contrarily, expression (7b) is the reconstruction using (possibly modified) contributions $\tilde{b}^j$. Both a^{j+1} and b^{j+1} are vectors with half

the number of components as a^j. Decomposition and reconstruction are preformed in a recursive manner. The transformation pair is shown more easily in diagrammatic form.

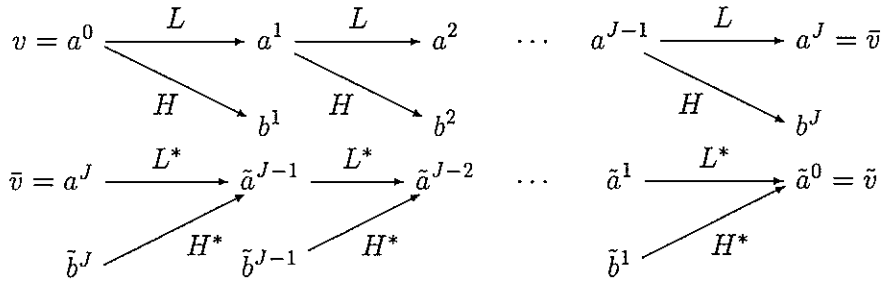

Setting $\tilde{b}^j = 0$ for $j \to 0$ removes small-scale perturbations which results in a 'blocky' velocity function. Contrarily $\tilde{b}^j = 0$ for $j \to J$ removes global trends while leaving high-frequency variations unperturbed.

EXAMPLE

We use a piece of an actual sonic-log as velocity function $v(z)$. The original profile (scales: 0-9), small-scale filtered versions (scales: x-9), and large-scale filtered versions (scales: 0-x,9) are shown in Figure 2. The corresponding reflection coefficients $|R(\omega)|^2$ are presented in Figure 3. For the small-scaled filtered velocity profiles, the largest reflection coefficients are typically obtained for the velocity function with the most detail, i.e., the original well-log. Removing small scales reduces the reflection amplitudes. However, removing the smallest scales hardly affects the reflectivity as a function of frequency. The effect of large-scale heterogeneity is different. Removing the largest scales typically increases the reflection amplitudes and strongly perturbes the behavior of the reflectivity.

Figure 4 presents the phase-slowness of the reflection coefficient as a function of frequency and scale. For nearly all scales, the phase-slownesses at low frequencies are the same. But the more small scales are removed, the lower the frequency becomes where the corresponding slowness begins to deviate from the one obtained for the complete well-log. Removing the large scales yields a different result. The behavior of the curves is nearly independent of scale content. However, each curve is shifted upwards by a constant slowness. The more large scales are removed, the greater the shift becomes. This effect can be interpreted as follows: the more large-scale velocity features are removed, the deeper the waves penetrate into the layer-stack. But the deeper the penetration, the longer the waves travel and hence, the greater the apparent slowness becomes.

The effect is even more pronounced for the reflection group-slowness shown in Figure 5 which is the derivative of the phase with respect to frequency. Its poles and zeros correlate with local minima of the reflection coefficient $|R|$. Removing the smallest scales perturbes the group-slowness. However, removing large scales or more than

just the smallest ones basically randomized the group-slowness. The plotted range of slownesses in Figure 5 is very small. In reality, some slownesses become unreasonable large while others might even become negative. Clearly, this is physically impossible. However, the corresponding amplitudes vanish which means that these waves are never observed. These seemingly unphysical slownesses have a simple explanation. For a vanishing reflection coefficients $|R(\omega)|^2$, the phase is not uniquely defined. Approaching a zero of the reflection coefficient from different directions in the complex ω-plane yields different limiting values.

Figure 6 shows the transmission coefficient $\xi_{0t}|T|^2$ as function of scale and frequency. By conservation of energy, we have $\xi_{0t}|T(\omega)|^2 = 1 - |R(\omega)|^2$ which means that Figure 6 is simply the complement of Figure 3. However, the effects of scale and frequency on transmission phase- and group-slownesses are completely different. Figure 7 shows the transmission phase-slownesses. The slownesses hardly depend on frequency which is to be expected since the transmission coefficients never vanish and hence no $\pm n\pi$ phase jump ever occurs. Removing scales increases the slowness. Furthermore, removing a small scale effects a small increment in slowness, while removing a large scale corresponds to a large slowness increment. Finally, the transmission group-slownesses are shown in Figure 8. The more scales are removed, the greater the group-slownesses but also the smaller their variabilities become. As stated, the transmission coefficient never vanishes in this example. However, there exist zeros of $|T(\omega)|$ in the complex ω-plane. Approaching such a zero along the real ω-axis still causes the phase to change since the phase varies continuously around the singularity at zero. The undulations of the group-slowness are the result these complex zeros.

CONCLUSIONS

The results show that transmission is mainly governed by some average, scale dependent velocity. The smaller the spectrum of scales, the greater the phase- and group-slownesses become. Most details of the slowness structure are not seen by the transmitted waves as expected for the self-averaging phase (Shapiro and Hubral, 1996). However, reflections are very sensitive even to small-scale variations of the slowness. Typically, the more small scales are excluded, the more the group- and phase-slownesses decrease. Contrarily, the more large scales are removed, the more the group- and phase-slownesses increase. Changes in the slownesses correlate with local minima of the reflection coefficient which might yield unreasonable group-slownesses. But these slownesses correspond to frequencies for which the reflection vanishes which means that they can never be observed.

ACKNOWLEDGMENTS

We thank Chevron Petroleum Technology Company for providing us with the well-logs. This work was supported by the Borehole Acoustics and Logging Consortium/Reservoir Delineation Consortia at the Massachusetts Institute of Technology.

References

Poggiagliolmi, E., Berkhout, A.J., and Boone, M.M, 1982, Phase unwrapping, possibilities and limitations, *Geophysical Prospecting, 30*, 281–291.

Shapiro, S. and Hubral, P., 1996, Elastic waves in finely layered sediments: The equivalent medium and generalized O'Doherty-Anstey formulas, *Geophysics, 61*, 1282–1300.

Shatilo, A.P., 1992, Seismic phase unwrapping: Methods, results, problems, *Geophysical Prospecting, 40*, 211–226.

Strang, G., 1989, Wavelets and dilatation equations: a brief introduction, *SIAM Review, 31*, 614–627.

Tribolet, J.M., 1977, A new phase unwrapping algorithm, *IEEE Transactions on Acoustic, Speech and Signal Processing, 25*, 170–177.

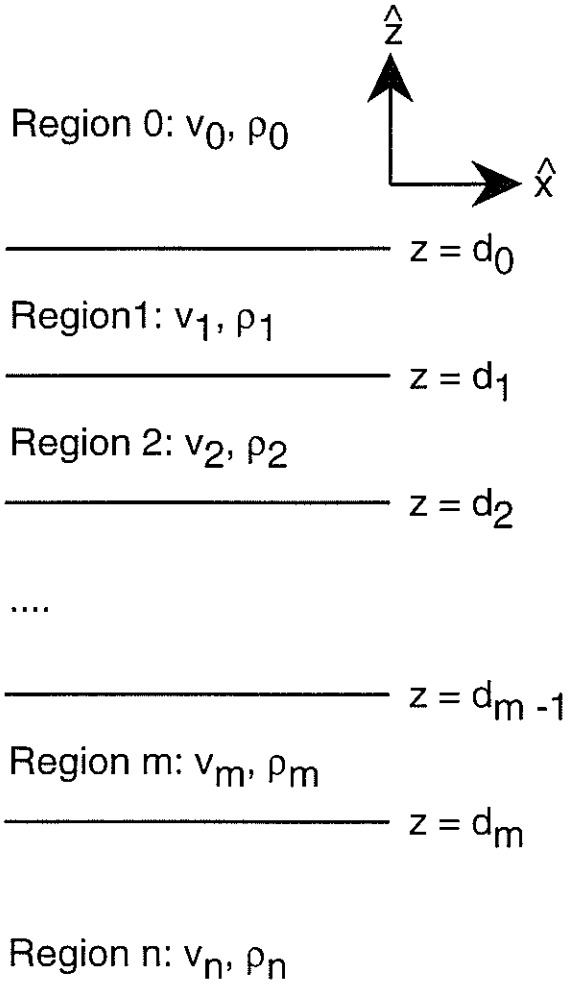

Figure 1: Schematic of geometry and its indexing.

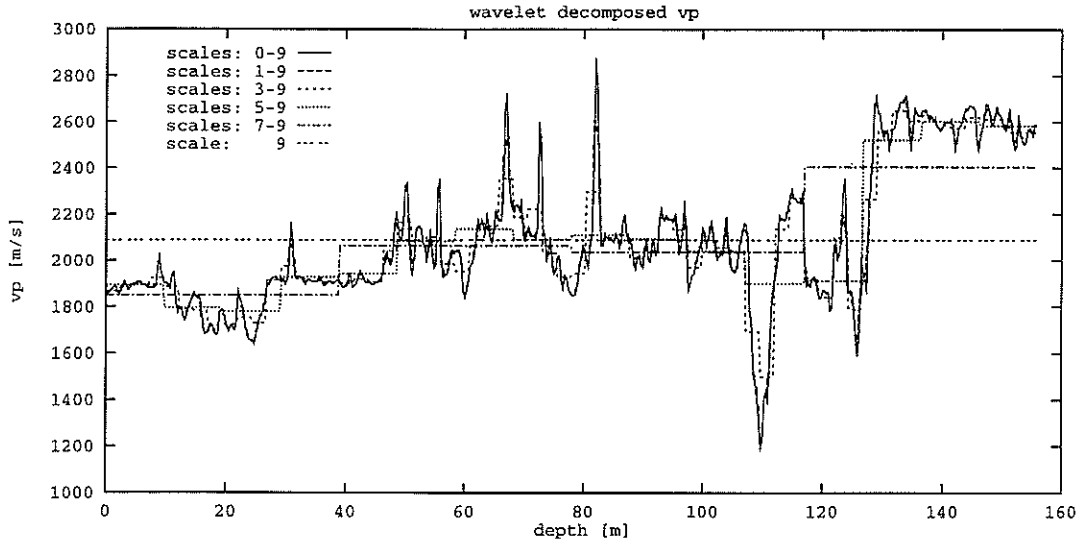

(a)

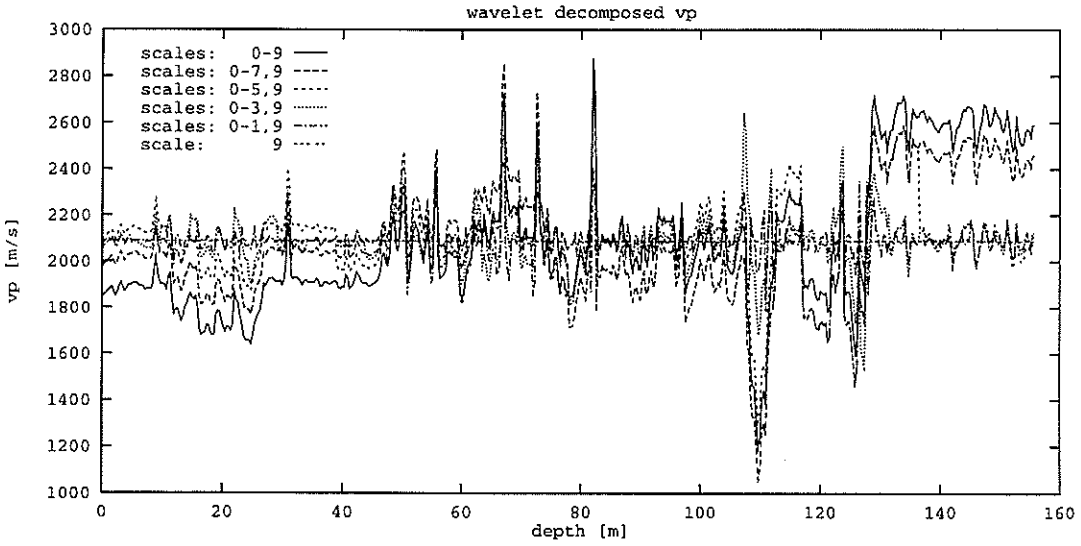

(b)

Figure 2: Wavelet filtered velocity profile with (a) small scales and (b) large scales removed.

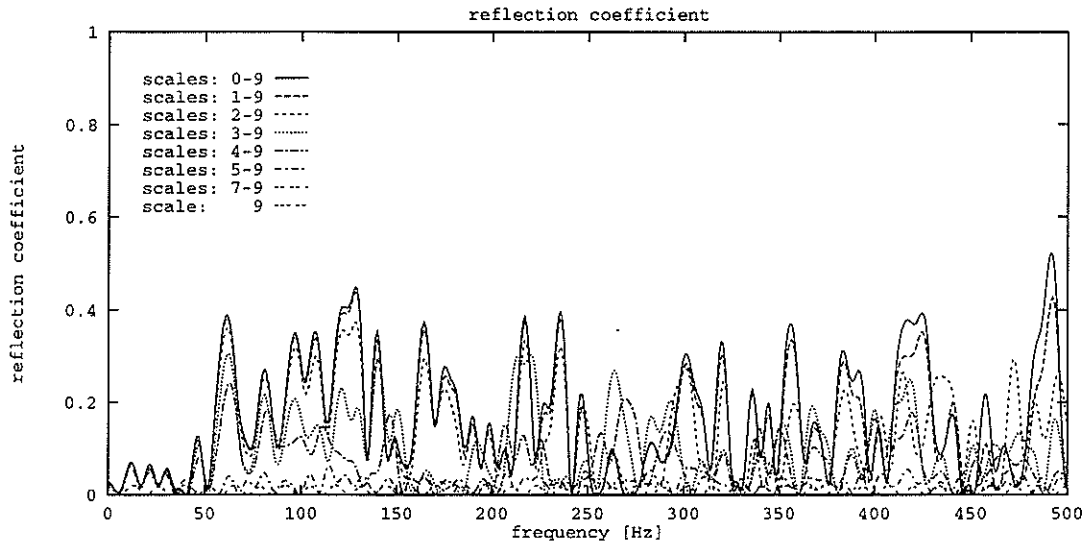

(a)

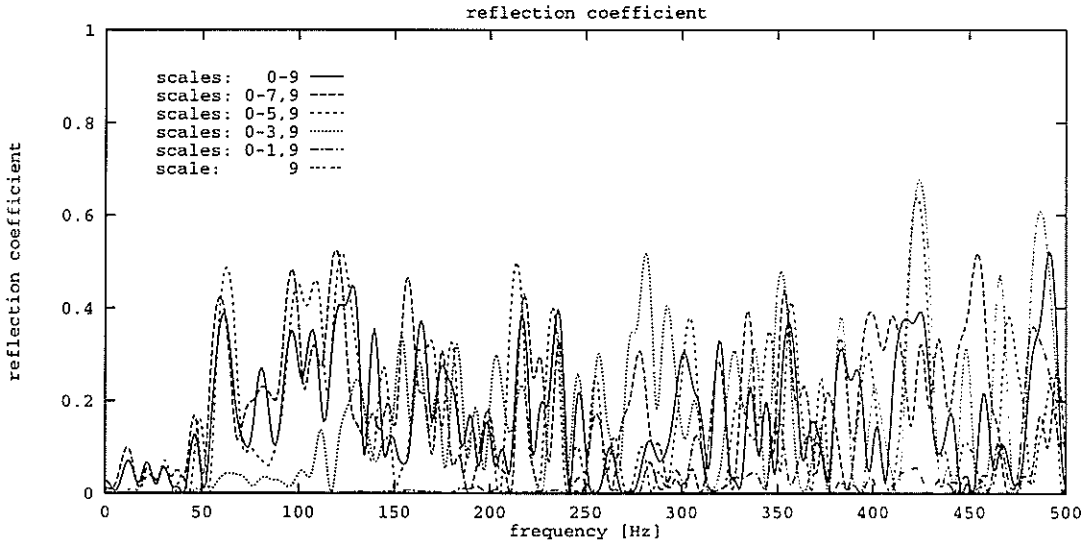

(b)

Figure 3: Magnitudes of reflection coefficient as functions of scale and frequency: (a) small scales removed, (b) large scales removed.

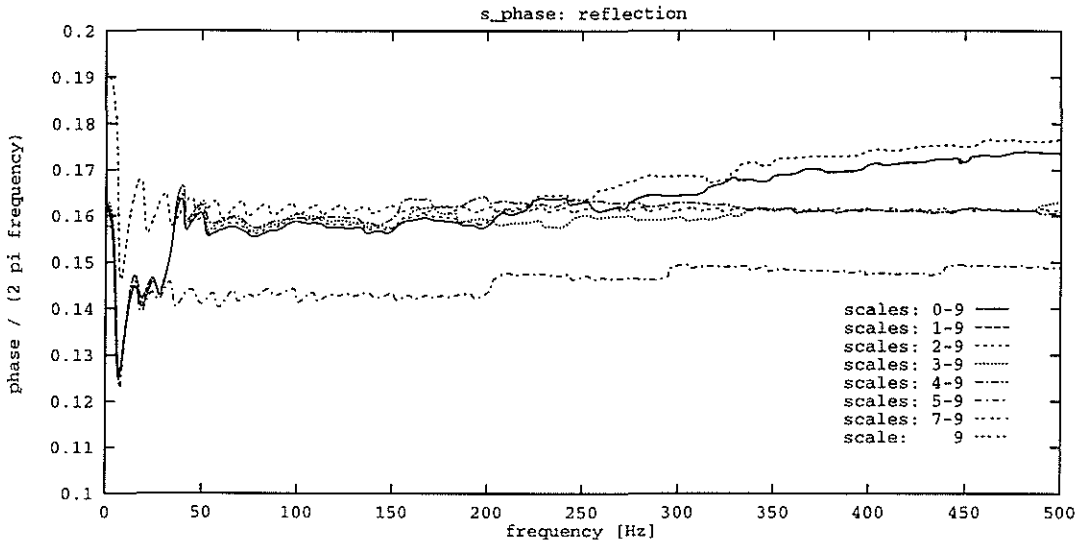

(a)

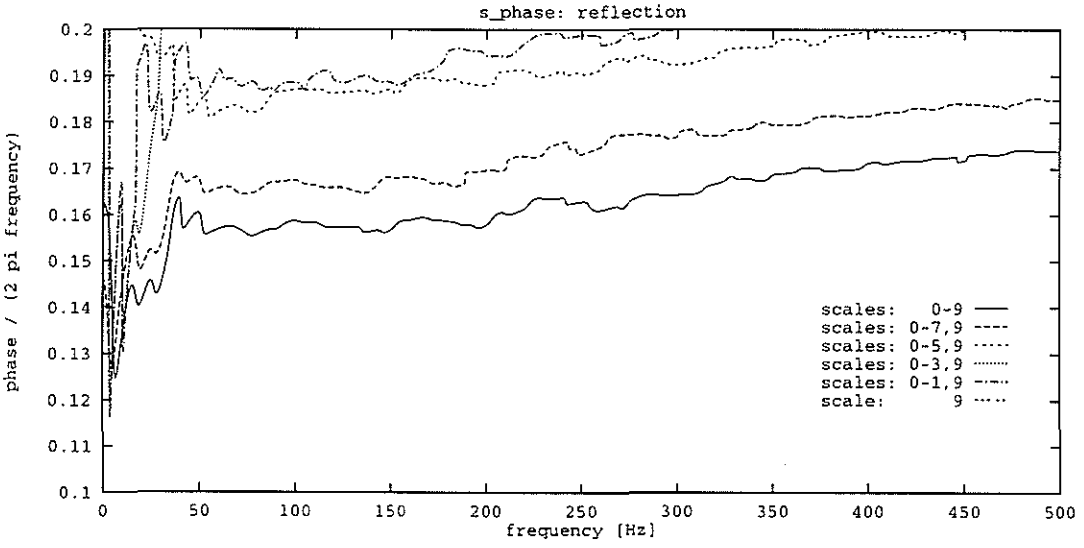

(b)

Figure 4: Reflection phase-slowness as function of scale and frequency: (a) small scales removed, (b) large scales removed.

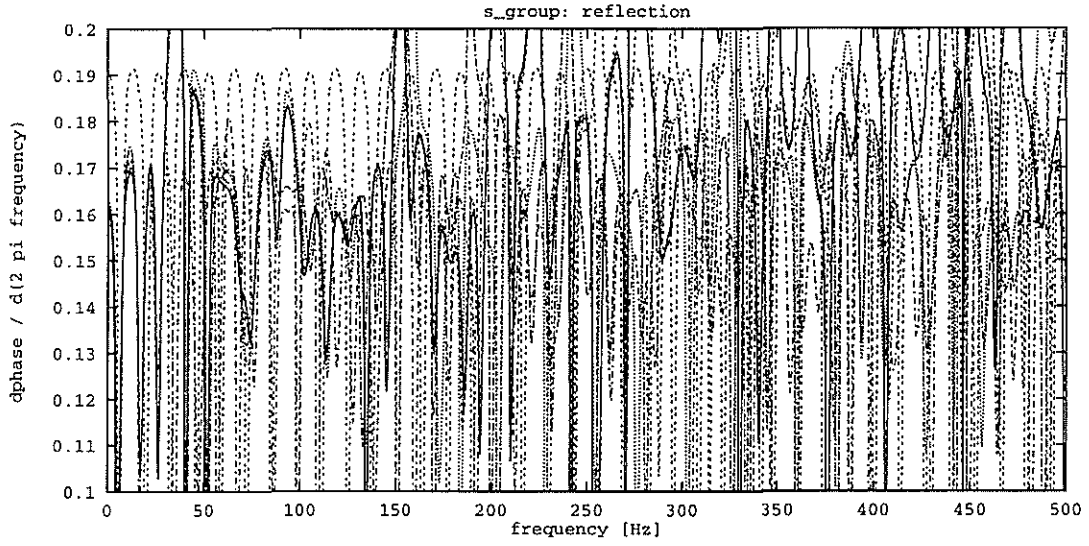

(a)

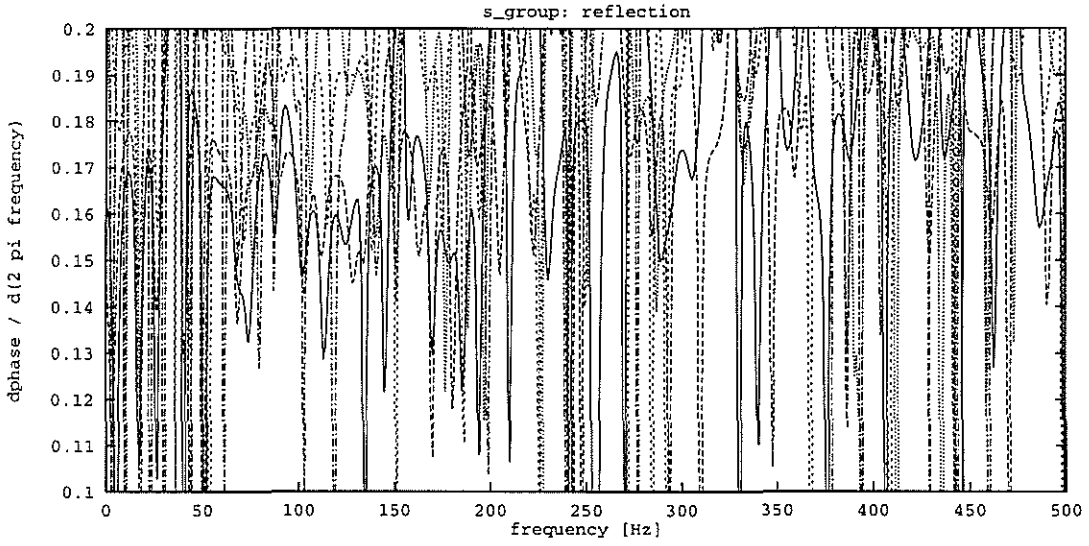

(b)

Figure 5: Reflection group-slowness as function of scale and frequency: (a) small scales removed, (b) large scales removed.

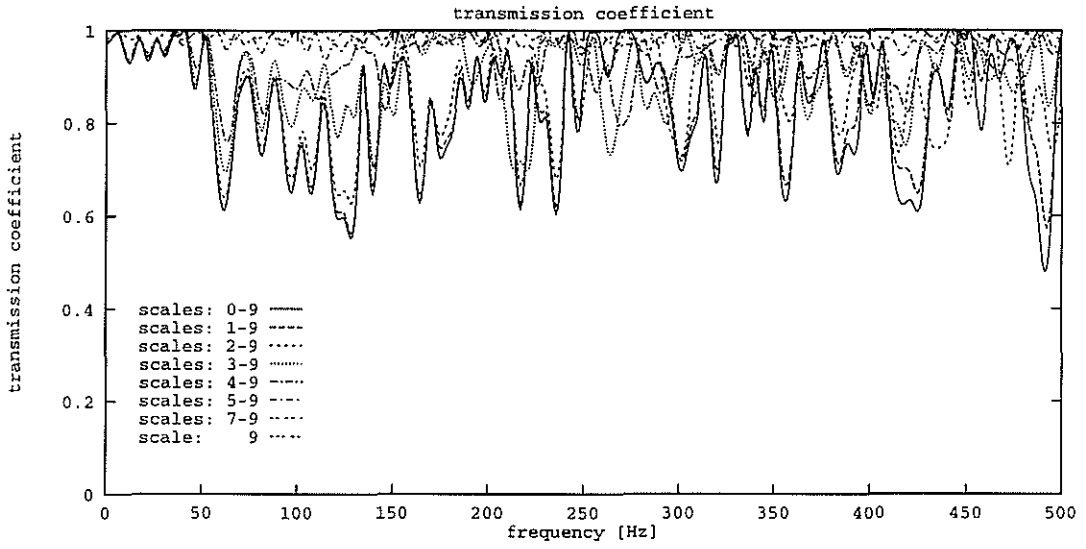

(a)

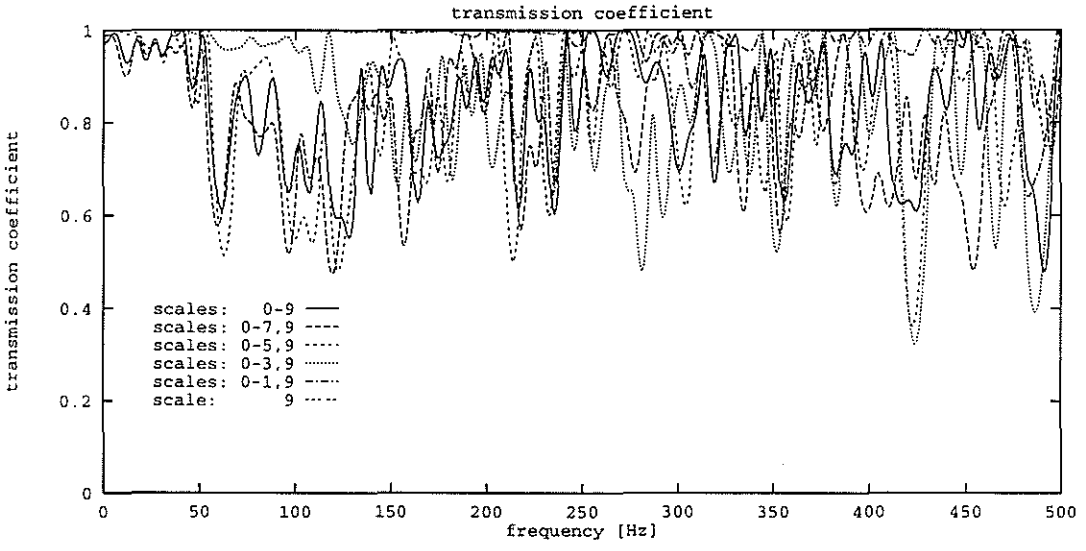

(b)

Figure 6: Magnitudes of transmission coefficient as functions of scale and frequency: (a) small scales removed, (b) large scales removed.

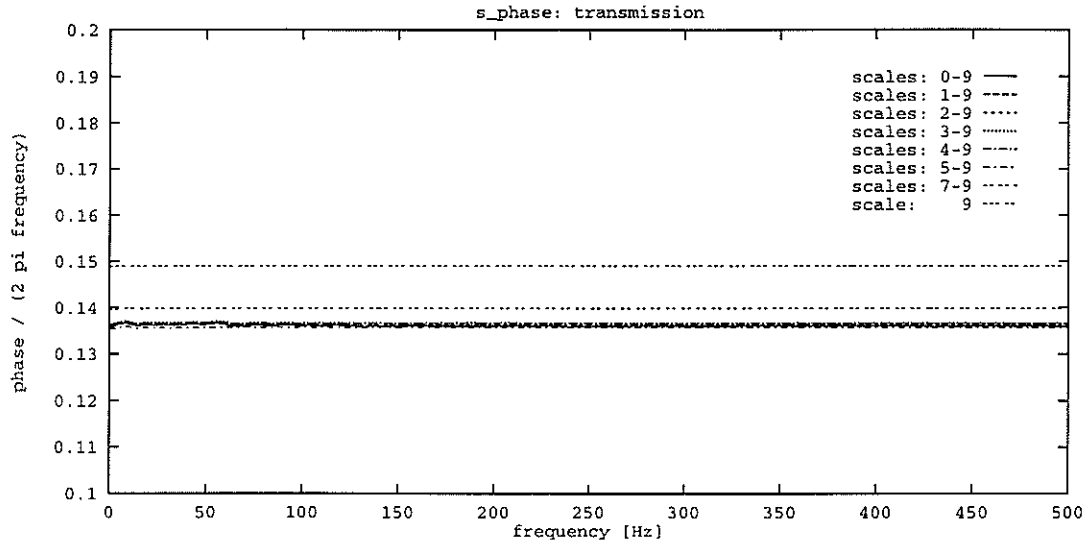

(a)

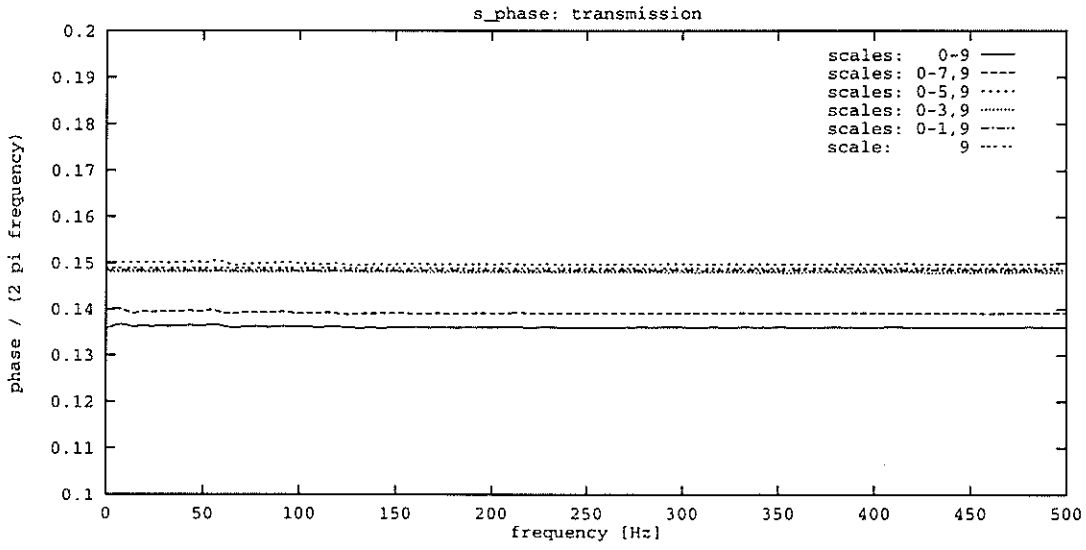

(b)

Figure 7: Transmission phase-slowness as function of scale and frequency: (a) small scales removed, (b) large scales removed.

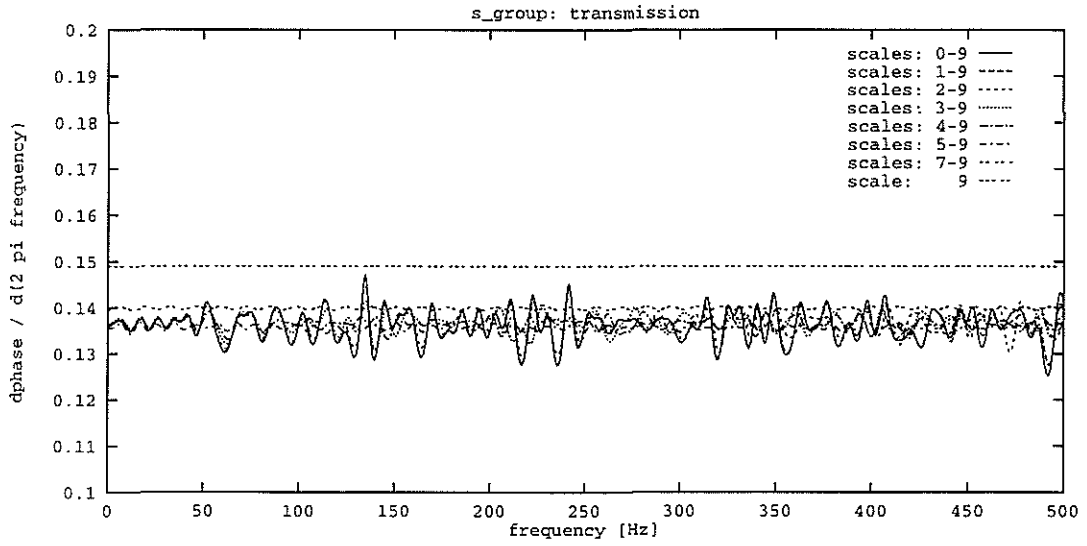

(a)

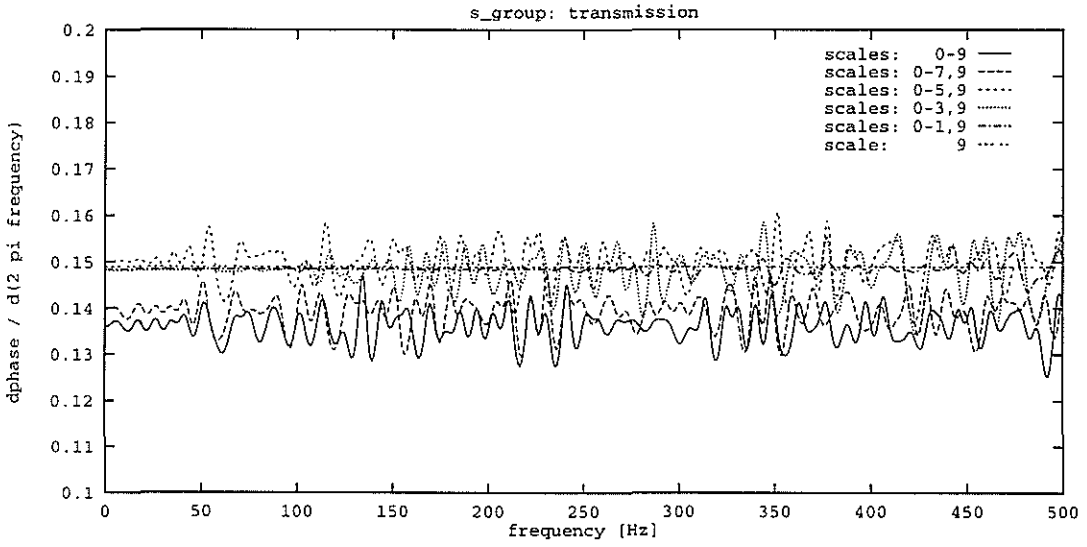

(b)

Figure 8: Transmission group-slowness as function of scale and frequency: (a) small scales removed, (b) large scales removed.